COBEM2015

ABCM Associação Brasileira de Engenharia e Ciências Mecânicas

23rd ABCM International Congress of Mechanical Engineering
December 6-11, 2015, Rio de Janeiro, RJ, Brazil

ONE-DIMENSIONAL GASEOUS CAVITATING FLOWS IN CONVERGING-DIVERGING NOZZLES

Rafael Dias Barreto, e-mail: faeldb1@hotmail.com
Felipe Bastos de Freitas Rachid, e-mail: rachid@vm.uff.br
Graduate Program in Mechanical Engineering (PGMEC)
Department of Mechanical Engineering (TEM)
Universidade Federal Fluminense
Rua Passo da Pátria, 156 , Niterói, RJ, 24210-240 - Brazil

Abstract. *This paper presents a numerical study about the gaseous cavitation in converging-diverging nozzles. The gaseous cavitation model used in the simulation has been recently proposed in the literature and is developed in the context of the thermodynamics of irreversible processes. By coherently contemplating the rate of energy dissipation associated with the gaseous cavitation, the model is capable to describe important irreversible effects observed in the flow of gas-liquid mixtures through small passages. Among them are the reduction of the wavefront speed and the occurrence of hysteresis phenomena.*

Keywords: *gaseous cavitation, thermodynamics of irreversible processes, converging-diverging nozzles.*

1. INTRODUCTION

Liquids are known to be able to absorb certain amount of gas in contact with their free surfaces. Through a diffusive process, the gas dissolves in the liquid and stays there, unless its temperature is raised beyond the boiling point or its pressure is lowered below the saturation pressure of the dissolved gas. In this last process, usually referred to as gaseous cavitation, the gas comes out of solution as small bubbles that are carried by the fluid flow stream as free gas forming a bubbly flow. Internal as well as external flows may be subjected to gaseous cavitation under steady and unsteady regimes. Boundary curvature of solid surfaces in contact with the liquids, vortices, turbulence and transient expansion waves are some typical examples of sources responsible for triggering the gas release phenomenon (Swaffield, 1972; Kranenburg, 1974; Wiggert & Sundquist, 1979; Baasiri and Tullis, 1983; Wylie, 1984; Chaudry et al., 1990; Hadj-Taieb & Lili, 1998; Kessal & Bennacer, 2005; Cannizzaro & Pezzinga, 2005)

Liquid-gas flows exists in various kinds of engineering facilities such as boiling heat transfer systems of nuclear power plants, aircraft fuel systems, oil pipelines, reactors in chemical industries and so on. Not only in the designing but also in maintenance of these facilities, sufficient knowledge of flow characteristics is crucially important to keep its security (Swaffield, 1972; Wylie & Streeter, 1993; Bergant et al., 2006).

This paper presents a numerical study about one-dimensional gas-liquid flows with gaseous cavitation in converging-diverging nozzles. To do so, a consistent thermodynamic model developed in the framework of the thermodynamics of irreversible processes is used (Freitas Rachid & Silva, 2013). The fluid is regarded as being a pseudo mixture of a liquid and a gas, both of them considered as compressible substances. These constituents are assumed to share the same fields of velocity and temperature, so that only one balance equation of momentum is used for the mixture as a whole. The gaseous volume fraction is treated as a state variable and its restriction is properly accounted in the constitutive relationships. In contrast to other existing models, the mass transfer process between the liquid and gaseous phases is consistently described as an irreversible process.

The capability of the model to properly describe gas-liquid flows in converging-diverging nozzles in the presence of gaseous cavitation is analyzed by means of numerical simulations. The numerical solutions were carried out for two different initial conditions associated with the initial gas volume fraction and two distinct saturation pressures. The results are compared with the case without cavitation. Besides the hysteresis phenomenon observed when the cavitation takes place, it is shown that a small increase in the saturation pressure can drastically increase the rate of energy dissipation and also the behavior of other important variables, such as the wavefront speed.

2. BALANCE EQUATIONS

Consider the one-dimensional isothermal homogeneous flow of a two-component, two-phase gas-liquid mixture through a converging-diverging nozzle in which mass exchange between the phases are susceptible to occur as a result of gaseous cavitation. Under the assumptions of thermal equilibrium and no slip between the phases, no fluid friction and absence

of gravitational effects, the following balance equations (in the Eulerian description) are sufficient to fully describe this thermo-mechanical problem:

$$A\frac{\partial}{\partial t}\left((1-\alpha)\rho_l\right)+\frac{\partial}{\partial x}\left((1-\alpha)\rho_l Au\right)=0, \tag{1}$$

$$A\frac{\partial}{\partial t}\left((1-\alpha)c\right)+\frac{\partial}{\partial x}\left((1-\alpha)cAu\right)=-A\Gamma, \tag{2}$$

$$A\frac{\partial}{\partial t}\left(\alpha\rho_g\right)+\frac{\partial}{\partial x}\left(\alpha\rho_g Au\right)=A\Gamma, \tag{3}$$

$$A\frac{\partial}{\partial t}\left(\rho u\right)+\frac{\partial}{\partial x}\left(\rho Au^2+pA\right)=\frac{\partial}{\partial x}\left(pA\right), \tag{4}$$

$$d:=-\dot{\Psi}-(\Psi+p)\frac{\partial u}{\partial x}-u\frac{p}{A}\frac{\partial A}{\partial x}\geq 0, \tag{5}$$

for $(x,t)\in(0,L)\times(0,+\infty)$, in which L stands for the nozzle length. In the these equations, u is the spatial velocity field of the mixture whose thermodynamic pressure is denoted by p. The concentration of dissolved gas in the liquid is represented by c, whereas ρ_l and ρ_g stand for the liquid and gas mass densities. Since by hypothesis the liquid and gaseous phases are assumed to coexist at a same material point at every time instant, the gas volume fraction α is subjected to the restriction $\alpha\in(0,1)$. It is implicit in the above equations that there is no vapor along with the gas. As a result, the mass density of the mixture ρ is the sum of the density of the phases weighted according to their volume fractions:

$$\rho=(1-\alpha)\left(\rho_l+c\right)+\alpha\rho_g. \tag{6}$$

As usual, the superimposed dot stands for the time material derivative and Ψ denotes the Helmholtz free energy per unit volume. With exception of the cross-sectional area A of the nozzle, which is supposed to be a known function of the spatial axial coordinate, all the other dependent variables are functions of the axial coordinate x and the time instant t. The rate of mass exchange between the gaseous and liquid phases as a result of the gaseous cavitation is represented by Γ. If the dissolved gas evolve from the liquid as a free gas, then $\Gamma>0$. On the other hand, if the free gas re-dissolves in the liquid phase, then $\Gamma<0$. Finally, if there is no mass transfer at all, then $\Gamma=0$ and the mass conservation principles associated with the dissolved gas and the free gas become independent from each other.

Equations (1) to (3) express the mass conservation principle for the liquid, the dissolved gas in the liquid phase and for the gaseous phase. Equation (4) expresses the momentum conservation principle for the mixture as a whole and Eq. (5) is a local version of the second law of the thermodynamics (SLT), which states that the rate of energy dissipation d must be non-negative. It distinguishes the possible processes ($d\geq 0$) from the impossible ones ($d<0$). The possible processes are classed as reversible as long as $d=0$ and irreversible when $d>0$.

To complete the problem description, constitutive relationships must be provided. They encompass expressions for p and Γ in such a way that Eq. (5) be satisfied no matter the external actions, the initial and the boundary conditions.

3. CONSTITUTIVE THEORY

The constitutive relations describing the macroscopic mechanical behavior of the liquid-gas mixture are derived in the framework of the thermodynamics of irreversible processes. In this theory, once the local state of the material has been characterized by means of an appropriate choice of the set of state variables, two thermodynamic potentials - the Helmholtz free energy and a pseudo-potential of dissipation - are sufficient to derive a complete set of constitutive equations. For this particular problem, we choose as state variables the local mass densities of the liquid ρ_l and the gas ρ_g, the concentration of dissolved gas in the liquid c, the gas volume fraction α and the absolute temperature θ. As we shall see, the restriction associated with α is treated in this work as a physical property in the constitutive equations. This approach has already been used by Freitas Rachid (2003) and Freitas Rachid (2006) in the modeling of cavitation in flows of compressible fluids and of surface tension effects in homogeneous liquid-gas flows, respectively.

3.1 Helmholtz free energy and state laws

Following the classic assumption of the thermodynamics of irreversible processes, the free energy per unit volume Ψ is supposed to be a function of the state variables ρ_l, ρ_g, c, α and θ. Since the fluid is regarded as a mixture of two constituents, its behavior is supposed to comprise a combination of the liquid and gas thermo-mechanical properties, taking α as a weighting factor. Thus, we choose

$$\Psi=\Psi\left(\rho_l,\rho_g,c,\alpha,\theta\right):=\Psi'\left(\rho_l,\rho_g,c,\alpha,\theta\right)+\overline{I}(\alpha), \tag{7}$$

in which

$$\Psi'\left(\rho_l,\rho_g,c,\alpha,\theta\right) \;:=(1-\alpha)\rho_l\Psi_l(\rho_l,\theta)+(1-\alpha)c\Psi_c(\theta)+\alpha\rho_g\Psi_g(\rho_g,\theta), \tag{8}$$

$$\overline{I}(\alpha):=\begin{cases}0 & \text{, if } \alpha\in(0,1)\\ +\infty & \text{, otherwise.}\end{cases} \tag{9}$$

In the above expression, Ψ' is a smooth function which describes the thermo-mechanical properties of the fluid whereas $\overline{I}(\alpha)$ represents the indicator function of the convex set $(0,1)$ (Moreau et al., 1988). The term $\overline{I}(\alpha)$ is the non-smooth parcel of the free energy and is included to take the internal constraint $\alpha \in (0,1)$ into account as a constitutive assumption. In other words, it prevents α from getting out of its admissible interval since it would be required a infinite amount of energy to do it.

The terms Ψ_l and Ψ_g represent the free energies per unit mass of liquid and gas, respectively. As suggested by its functional dependence, these free energies are supposed to represent the thermo-mechanical behavior of the liquid and the gas as if they were single constituents. Finally, the term Ψ_c denotes the free energy per unit mass of dissolved gas which is incorporated in the free energy of the mixture to take the release and absorption of gas into account. For the sake of simplicity, it is assumed as a constitutive hypothesis that Ψ_c depends on the temperature only. According to the theory presented in Freitas Rachid & Silva (2013), the following forms for these free energies are assumed:

$$\Psi_l = \Psi_l(\rho_l,\theta) := -C_l\theta\log\theta + a_l^2\left(\frac{\rho_l^o}{\rho_l} + \log\rho_l\right), \tag{10}$$

$$\Psi_g = \Psi_g(\rho_g,\theta) := -C_g\theta\log\theta + a_g^2\log\rho_g, \tag{11}$$

$$\Psi_c = -C_g\theta\log\theta + a_g^2\log\frac{p_s}{a_g^2} + a_g^2. \tag{12}$$

In the above expressions, C_l and C_g are assumed to be constants. They represent the specific heats at constant volume of the liquid and free gas, respectively. The material parameters ρ_l^o, a_l^2 and a_g^2 are temperature dependent, being the last two the square of the isothermal wavefront propagation velocities in the pure liquid and pure gas, respectively. In Eq. (12) p_s stands for the saturation pressure which depends on the temperature only, i. e., $p_s = p_s(\theta)$.

The state laws for the fluid, relating the reversible components of the thermodynamic forces to the state variables, are obtained from the free energy potential and defined as follows:

$$B^{\varrho_l} := \frac{\partial\Psi'}{\partial\rho_l} = (1-\alpha)\big(\Psi_l + \frac{p_l}{\rho_l}\big) = (1-\alpha)g_l, \tag{13}$$

$$B^{\varrho_g} := \frac{\partial\Psi'}{\partial\varrho_g} = \alpha\big(\Psi_g + \frac{p_g}{\rho_g}\big) = \alpha g_g, \tag{14}$$

$$B^{c} := \frac{\partial\Psi'}{\partial c} = (1-\alpha)\Psi_c, \tag{15}$$

$$B^{\alpha} := \frac{\partial\Psi'}{\partial\alpha} + h, \quad \text{with} \quad h \in \partial_\alpha\overline{I}(\alpha), \tag{16}$$

in which;

$$\frac{\partial\Psi'}{\partial\alpha} = \rho_g\Psi_g - \rho_l\Psi_l - c\Psi_c, \tag{17}$$

$$p_l := \rho_l^2\frac{\partial\Psi_l}{\partial\rho_l} = a_l^2\,(\rho_l - \rho_l^o) \quad \text{and} \quad p_g := \rho_g^2\frac{\partial\Psi_g}{\partial\rho_g} = a_g^2\rho_g. \tag{18}$$

In the above equations, p_l and p_g stand for the liquid and gas partial pressures, respectively. The term h in Eq. (16) is an element of the sub-differential set $\partial_\alpha\overline{I}(\alpha)$ (also called generalized derivative) with respect to α of the convex function $\overline{I}(\alpha)$. The sub-differential of the indicator function $\overline{I}(\alpha)$ at α is given by the set (Ekeland & Teman, 1976; Moreau et al., 1988);

$$\partial_\alpha\overline{I}(\alpha) := \{h \in \mathbb{R} | \overline{I}(\alpha^\star) - \overline{I}(\alpha) \geq h(\alpha^\star - \alpha); \quad \forall\alpha^\star \in (0,1)\}. \tag{19}$$

A straightforward calculation shows that $\partial_\alpha\overline{I}(0<\alpha<1) = \{0\}$ and $\partial_\alpha\overline{I}(\alpha) = \emptyset$ if $\alpha \notin (0,1)$. The restriction $\alpha \in (0,1)$ is effectively taken into account through the constitutive law Eq. (16), since this relation implies that the sub-differential $\partial_\alpha\overline{I}(\alpha)$ is not empty.

Keeping in mind that time derivatives must be left derivatives in order to cope with the principle of determinism, it comes out that the material time derivative $\dot{\Psi}$ which appears in Eq. (5) can be written for $\alpha \in (0,1)$ as:

$$\dot{\Psi} = \frac{\partial\Psi'}{\partial\rho_l}\dot{\rho}_l + \frac{\partial\Psi'}{\partial\rho_g}\dot{\rho}_g + \frac{\partial\Psi'}{\partial c}\dot{c} + \frac{\partial\Psi'}{\partial\alpha}\dot{\alpha}. \tag{20}$$

When the above result is used in Eq. (5) along with the state laws Eqs. (13-16), Eq. (5) can be rewritten as:

$$d := -(\Psi + p)\frac{\partial u}{\partial x} - B^{\rho_l}\dot{\rho}_l - B^c\dot{c} - B^{\rho_g}\dot{\rho}_g - B^\alpha\dot{\alpha} \geq 0. \tag{21}$$

To obtain a complete set of constitutive equations, it suffices to specify a pseudo-potential of dissipation from which complementary laws are derived in such a way that the local version of the SLT given by Eq. (5) or (21) is always verified, regardless the initial and boundary conditions.

3.2 Pseudo-potential of dissipation and complementary laws

To introduce the irreversible behavior of the gas-liquid mixture, and also to ensure that the SLT is always satisfied, we assume that there exists a pseudo-potential of dissipation Φ, which is an objective, convex and differentiable function of B^Γ. We implicitly assume here, as it has been stated before, that the fluid is perfect, i.e., there is no viscosity. Moreover, the pseudo-potential $\Phi = \Phi(B^\Gamma; \alpha, c, \theta)$ is assumed to have the following properties:

$$\Phi(B^\Gamma; \alpha, c, \theta) \geq 0 \quad \text{and} \quad \Phi(0; \alpha, c, \theta) = 0, \tag{22}$$

whatever the values of B^Γ, α, c and θ.

The additional information associated with the dissipative behavior of the fluid is obtained from Φ through the following complementary law:

$$\Gamma := \frac{\partial \Phi}{\partial B^\Gamma}. \tag{23}$$

In addition, if the rate of energy dissipation d is supposed to have the form for $\alpha \in (0, 1)$,

$$d := B^\Gamma \Gamma, \tag{24}$$

then we get from the convexity property of Φ that, for any actual evolution (Berger, 1977):

$$d := B^\Gamma \Gamma \geq \Phi(B^\Gamma; c, \alpha, \theta) - \Phi(0; c, \alpha, \theta). \tag{25}$$

In view of Eq. (22), it is easy to see that $d \geq 0$ for any actual evolution of the fluid and so the SLT given by the inequality Eq. (5) is always satisfied.

From the mechanical viewpoint, Eq. (24) establishes that the dissipated energy rate is due to the gaseous cavitation process only. The constitutive assumptions made so far are sufficient to partially characterize the mechanical behavior of the pseudo-fluid. Since the mass balance equations given by Eqs. (1,2,3) define subspaces of the linear space spanned by u, $\dot{\rho}_l$, $\dot{\rho}_g$, $\dot{c}$ and $\dot{\alpha}$, then in order that Eq. (21) be equal to Eq. (24) for any actual evolution it is possible to prove that (Freitas Rachid & Silva, 2013), for $\alpha \in (0, 1)$, one must have the following relationships among the thermodynamic forces:

$$p = p_l = p_g, \tag{26}$$

$$B^\Gamma = \Psi_c - g_g. \tag{27}$$

The above relationships establish that the mixture pressure is equal to the partial pressures of the liquid and the free gas and that the thermodynamic force associated with the rate of gas mass transfer between the liquid and gaseous phases is equal to the difference of the free energies in these two phases.

In the sequel, we assume the following simple and appropriate choice for Φ:

$$\Phi(B^\Gamma; \alpha, c, \theta) := \frac{\beta_r}{2n_r} \langle B^\Gamma \rangle^{2n_r} + \frac{\beta_a}{2n_a} \langle -B^\Gamma \rangle^{2n_a}. \tag{28}$$

in which $\beta_k = \beta_k(c, \theta)$ and $n_k = n_k(\theta)$, with $k \in \{a, r\}$, are positive material constants, with $n_k > 1/2$, associated with the gas release ($k = r$) and gas absorption ($k = r$) phenomena. The term $\langle \chi \rangle$ stands for the maximum value between zero and χ, i. e., $\langle \chi \rangle := \max\{0, \chi\}$. Equation (28) satisfies the conditions set forth before, and so the SLT given by Eq. (21) is unconditionally satisfied. As a result, based on Eqs. (23), (26-27) and (28), the specific choices expressed by Eq. (10-28) give rise to the following constitutive equation:

$$\Gamma = \beta_r \left(a_g^2\right)^{2n_r - 1} \langle \log \frac{p_s}{p} \rangle^{2n_r - 1} - \beta_a \left(a_g^2\right)^{2n_a - 1} \langle \log \frac{p_s}{p} \rangle^{2n_a - 1}, \tag{29}$$

in which $a_g = a_g(\theta)$, $\beta_k = \beta_k(c, \theta)$ and $n_k = n_k(\theta)$, with $k \in \{a, r\}$.

Due to the nature of the functional relationship employed in Eq. (29), it is easy to note that Γ can be such that $\Gamma \geq 0$ as well as $\Gamma \leq 0$. In other words, the gas release phenomenon is considered as well as the reverse process of gas absorption. The mass transfer can take place from the gas dissolved in the liquid to the free gas in suspension in the fluid and vice-versa. Although the characteristic time of the gas absorption phenomenon is much longer than the gas release one, both processes can be accounted for in the proposed theory within a same context. Equation (29) states that gas will evolve of the liquid whenever the mixture pressure falls below the saturation pressure ($p < p_s$). On the other hand, gas will dissolve in the liquid whenever the liquid pressure is greater than the saturation pressure ($p > p_s$). Both situations are in accordance with the experimental results.

The saturation pressure, which is a constitutive parameter in the model proposed herein, is related to the saturation concentration of dissolved gas in the liquid by the Henry's law (Sander, 1999). This law states that the amount of gas dissolved in a liquid is directly proportional to the partial pressure of that gas in the gaseous phase in contact with the liquid, at thermo-mechanical equilibrium, i.e., $p_s = k_{\mathrm{H}} c_s$, in which $k_{\mathrm{H}} = k_{\mathrm{H}}(\theta)$ is the temperature-dependent Henry's law proportionality constant, for a specific gas-liquid pair under consideration (Sander, 1999).

4. NUMERICAL SIMULATIONS

To get a better understanding about the gaseous cavitation on gas-liquid mixture flows we take as a primary example the steady-state flow through a converging-diverging nozzle. In this problem, the gaseous cavitation is induced by the pressure reduction that takes place as a result of the area contraction. In spite of being simple from the mechanical viewpoint, this specific problem counts with scarce experimental data available in the literature, at least when gaseous cavitation is the central matter. Aiming to adhere as much as possible to the actual physical situation, we appeal to the existing experimental data of Zielke et al. (1990) about gaseous cavitation, which in turn is not devoted specifically to steady-state flows in converging-diverging nozzles. Although Zielke's data have been raised in the context of unsteady flows, they can be used to adjust the material coefficients of the constitutive model proposed in the past section, as it has been shown in Freitas Rachid & Silva (2013).

On the other hand, to reduce the three-dimensionality effects of the flow, we appeal to the nozzle geometry employed in the experimental and theoretical work of Dorofeeva et al. (2009), which was used to investigate not the gaseous but the vaporous cavitation (the liquid-vapor transformations) of aviation fuels through narrow passages.

By considering the Zielke's data, which rules out the possibility of the free gas re-dissolves in the liquid, and the Dorofeeva's nozzle geometry, the governing equations under steady-state flow are reduced to:

$$\frac{dp}{dx} = \frac{\dot{m}}{(\mathrm{M}^2-1)}\left(\frac{\Gamma}{A\rho_g} - \frac{u}{A^2}\frac{dA}{dx}\right), \tag{30}$$

$$\frac{du}{dx} = -\frac{A}{\dot{m}}\frac{dp}{dx}, \tag{31}$$

$$\frac{d\alpha}{dx} = \left(1 - \frac{\rho u^2}{\rho_g a_g^2}\right)\frac{\alpha}{\rho u^2}\frac{dp}{dx} + \frac{1}{u\rho_g}\Gamma - \alpha\frac{1}{A}\frac{dA}{dx}, \tag{32}$$

$$\frac{dc}{dx} = \frac{c}{(1-\alpha)}\frac{d\alpha}{dx} + \frac{c}{\rho u^2}\frac{dp}{dx} - \frac{\Gamma}{(1-\alpha)u} - c\frac{1}{A}\frac{dA}{dx}, \tag{33}$$

for $x \in (0, L)$, in which $\dot{m} = \rho u A$, which is a constant, is the mass flow rate trough the nozzle and $\mathrm{M} := u/a$ stands for the Mach number; being a the wavefront speed in the gas-liquid mixture:

$$a = \left[\frac{a_l^2\rho_l a_g^2\rho_g}{\rho\big(a_l^2\rho_l\alpha + a_g^2\rho_g(1-\alpha)\big)}\right]^{1/2}. \tag{34}$$

The rate of mass transfer Γ and the the cross-sectional area of the nozzle $A := y(x)h$, with h =1.6mm being the nozzle depth, are given by:

$$\Gamma = k(\mathrm{Re})^{0.86}\beta_r\langle\log\frac{p_s}{p}\rangle^{2n_r-1}, \quad \text{with} \quad k = \frac{7.1\times10^{-11}}{D_h^2}[\mathrm{kgm}^3/\mathrm{s}] \tag{35}$$

$$y(x)[mm] = \begin{cases} a_5^{(c)}x^5 + a_4^{(c)}x^4 + a_3^{(c)}x^3 + a_2^{(c)}x^2 + a_1^{(c)}x + a_0^{(c)}, & \text{if} \quad 0 \le x[\mathrm{mm}] \le 25.4 \\ 1.59, \quad \text{if} \quad 25.4 < x[\mathrm{mm}] < 31.8 \\ a_5^{(d)}x^5 + a_4^{(d)}x^4 + a_3^{(d)}x^3 + a_2^{(d)}x^2 + a_1^{(d)}x + a_0^{(d)}, & \text{if} \quad 31.8 \le x[\mathrm{mm}] \le 127 \end{cases} \tag{36}$$

in which $\mathrm{Re} := (\rho_l U D_h)/\mu_l$ is the Reynolds number; with $D_h := 4A/P$ being the hydraulic diameter, U the mixture velocity and P the wetted perimeter, all of them evaluated at the nozzle throat.

The overall length of the nozzle, L, is 127 mm. The nozzle throat area is constant from $x = 25.4$ mm to $x = 31.8$ mm. The inlet and exit heights, $y(x = 0\mathrm{mm})$ and $y(x = 127\mathrm{mm})$, are both 19 mm and the throat height is 1.59 mm. This gives a nozzle inlet-to-throat area ratio of 12:1. The coefficients of the polynomials in Eq. (36), which describe the converging and diverging sections of the nozzle height as a function of the axial coordinate, are presented in Table 1.

Table 1. Coefficients of the polynomials given by Eq. (36) which characterize the nozzle profile.

	$i=5$	$i=5$	$i=3$	$i=2$	$i=1$	$i=0$
$a_i^{(c)}$	-6.4367804E-6	+4.1349816E-4	-6.4900889E-3	-2.2789376E-2	-1.6195205E-2	+1.8999921E+1
$a_i^{(d)}$	+1.0820115E-8	-4.3056382E-6	+5.9625754E-4	-3.3277792E-2	+8.0739920E-1	-5.5563366E+0

The material coefficients for Eq. (35) associated with the gas release phenomenon in the gaseous cavitation for a air-water mixture at room temperature are presented at Table 2 for two distinct saturation pressures of p_s=52 kPa and p_s=125 kPa. These coefficients have been adjusted in Freitas Rachid & Silva (2013), based on the experimental results of Zielke et al. (1990). The dissolved gas concentrations, which are associated with these saturation pressures through the Henry's law, are also displayed in Table 2.

Table 2. Material coefficients for Eq. (35) which characterize gas release phenomenon in the gaseous cavitation for two distinct saturation pressures.

p_s (kPa)	c_s (kg/m^3)	β_r (–)	$2n_r - 1$ (–)
52	0.021	0.00100	4.445
125	0.050	0.03088	3.420

As it can be seen in Eq. (34), the wavefront speed a depends not only on the gas volume fraction α and on the pressure p through the equations of state for the liquid and gas, but also on the concentration of dissolved gas c which appears in the mass density of the mixture ρ (see Eq. (6)). However, since in practice $c \ll \rho_l$ (c/ρ_l is of the order of 10^{-5}) the dependence of a on c is insignificant and therefore can be disregarded. As a result, Eq. (34) looks like exactly the classical expression derived in the pioneering work of Wood (1930).

The influence of the gas volume fraction and pressure on the wavefront speed can be visualized in Fig. 1, which has been plotted using Eq. (34) for an air-water mixture at room temperature ($a_l = 1485$m/s, $\rho_l^o = 997.98$kg/m^3 and $a_g = 290$m/s). It can be seen that even for small values of the gas volume fraction, the wavefront speed is drastically reduced as the pressure in the mixture drops below 100 kPa until the vapor pressure 2.334kPa. As we will see later, the gas release process acts by reducing even further the wavefront speed, what justifies its inclusion on the modeling when wave propagation phenomena become a relevant feature.

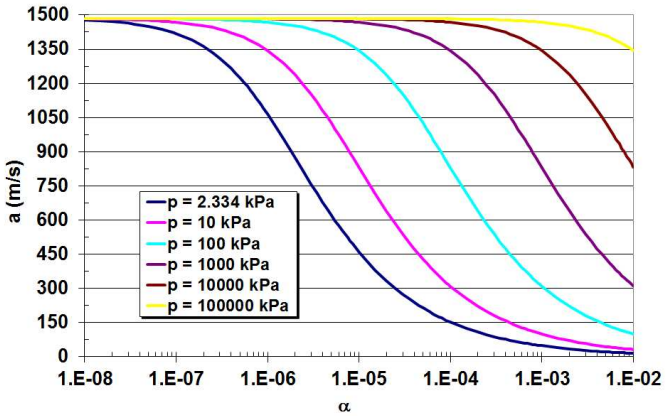

Figure 1. Wavefront speed a as a function of the gas volume fraction at different pressures p =2.34; 10; 100; 1000; 10,000; 100,000 kPa for an waterŰair mixture at room temperature

To access the effects of the gas release process on the flow of a gas-liquid mixture through the nozzle characterized before, the system of ordinary differential equations given by Eq. (30) to (33) is solved numerically for a air-water mixture at room temperature. To ensure that the gas volume fraction will not attain excessive high values inside the nozzle so that bubble dynamics will not become relevant and to guarantee that the flow will not become sonic at the throat giving rise to the possibility of standing shock waves at the divergent section, only low values of gas volume fractions are considered along with a combination of a low fluid velocity and a relative high pressure as initial conditions at the nozzle inlet. Thus, as initial conditions we have considered all possible combinations of the following values:

$$p(x=0) = p_o = 303.98 \text{ kPa}, \quad u(x=0) = u_o = 2.0 \text{ m/s}, \tag{37}$$

$$\alpha(x=0) = \alpha_o = \begin{cases} 10^{-8} \\ 10^{-4} \end{cases} \quad c(x=0) = c_o = \begin{cases} 0.021 \text{ kg/m}^3 & (p_s = 52\text{kPa}) \\ 0.050 \text{ kg/m}^3 & (p_s = 125\text{kPa}) \end{cases} . \tag{38}$$

The approximated numerical solution to the initial-value problem formed by Eq. (30) to (33) along with Eq. (37-38) was carried out by using the classic Gear's method, with initial spatial mesh sizes of 0.635 mm and a tolerance of the order of 10^{-5}. Gear's method is a multi-step method up to fifth order and is specially designed to deal with stiff differential equations.

In what follows, we present the numerical results obtained by considering the initial conditions given in Eq. (37) with $\alpha_o = 10^{-8}$ and $\alpha_o = 10^{-4}$, for two different saturation pressures $p_s = 52$kPa and $p_s = 125$kPa, which correspond to c_o =0.021 kg/m^3 and c_o =0.050 kg/m^3, respectively. To better highlight the effects of the gas release on the fluid flow, numerical simulations have also been carried out without taking the cavitation phenomenon into account, by setting $\Gamma = 0$ in Eqs. (30, 32, 33). The normalized responses of pressure $p^+ := p/p_o$, velocity $u^+ := u/u_o$, gas volume fraction $\alpha^+ := \alpha/\alpha_o$, wavefront speed $a^+ := a/a_o$ and gas mass fraction $f^+ := f/f_o$ (with $f := (\alpha\rho_g)/\rho$) as a function of the normalized position along the nozzle $x^+ := x/L$ are plotted in Figs. 2 and 3 for $\alpha_o = 10^{-8}$ and $\alpha_o = 10^{-4}$, respectively.

In order to help the interpretation of these curves, the upper half nozzle profile has also been displayed with a black line in these figures.

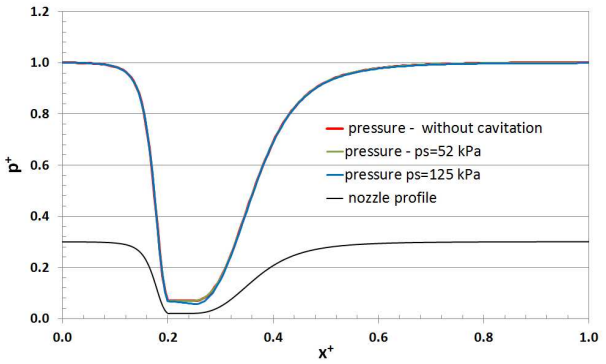

(a) Normalized pressure vs normalized position

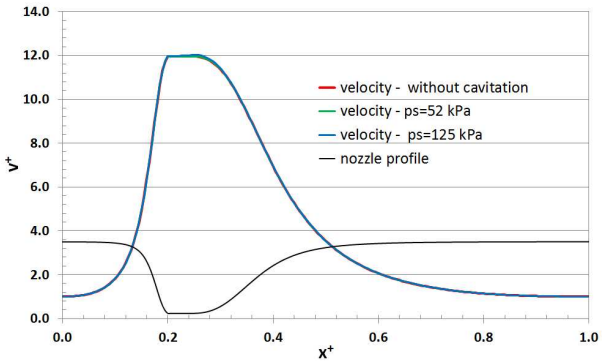

(b) Normalized velocity vs normalized position

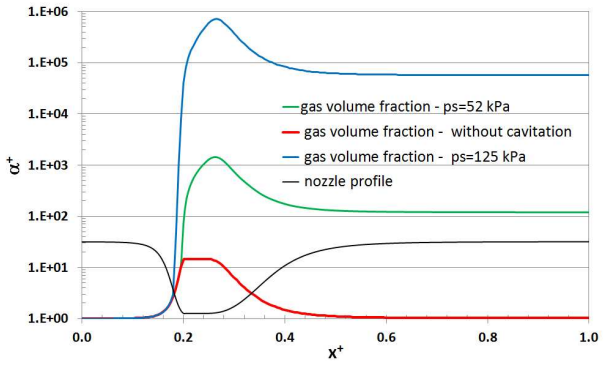

(c) Normalized gas volume fraction vs normalized position

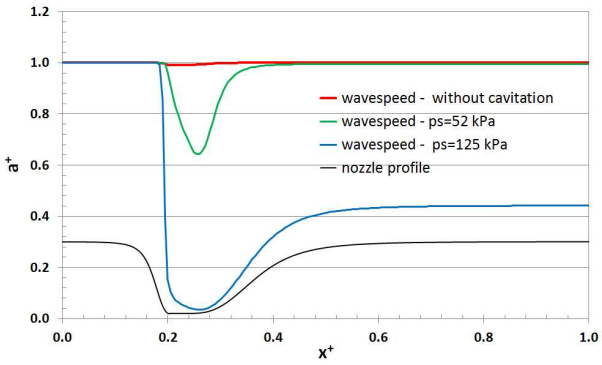

(d) Normalized wavefront speed vs normalized position

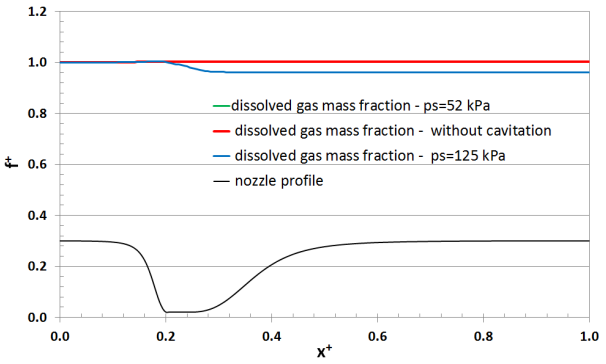

(e) Normalized dissolved gas mass fraction vs normalized position

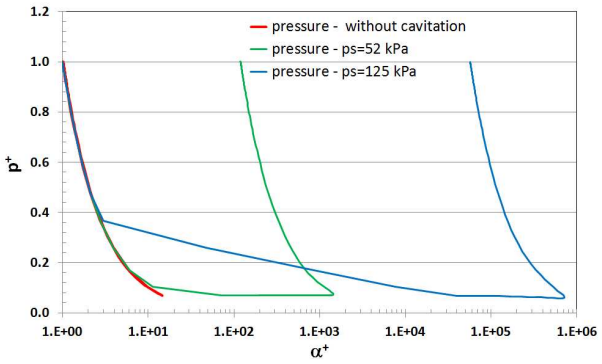

(f) Normalized pressure vs normalized gas volume fraction

Figure 2. Mechanical response of a water-air mixture at room temperature flowing in a converging-diverging nozzle for three different situations: i) without cavitation; ii) with cavitation for a saturation pressure p_s=52 kPa and iii) with cavitation for a saturation pressure p_s=125 kPa. The inlet gas volume fraction is α_o=10^{-8}.

As it can be seen in Fig. 2(a) and Fig. 2(b), the pressure and velocity responses for both saturation pressures p_s = 52kPa and p_s = 125kPa are almost the same of that observed for the flow without cavitation, except at a small site of the nozzle throat exit. As expected, the velocity increases through the convergent section, attains its maximum at the nozzle throat and then decreases along the divergent section. An inverse behavior is observed for the pressure response. The differences between the cavitating and non-cavitating responses become apparent in the plots of the normalized gas volume fraction and wavefront speed presented in Fig. 2(c) and Fig. 2(d). When there is no cavitation, there is no dissipative mechanism. The gas volume fraction becomes ten times greater at the nozzle throat but restores to its initial value at the nozzle exit (see Fig. 2(c)). For the cavitating flows, the greater the saturation pressure is, the higher the gas volume fraction becomes at the nozzle throat. At this location, the gas volume fraction is one thousand and one

million greater than the initial value α_o for $p_s = 52$kPa and $p_s = 125$kPa, respectively. In contrast to the non-cavitating responses, the gas volume fraction does not get back to its initial value at the divergent section of the nozzle. In the absence of cavitation, due to the slight variation of the gas volume fraction and pressure, the wavefront speed remains practically unaltered throughout the nozzle (around $a_o = 1480$m/s), as it can be seen in Fig. 2(d).

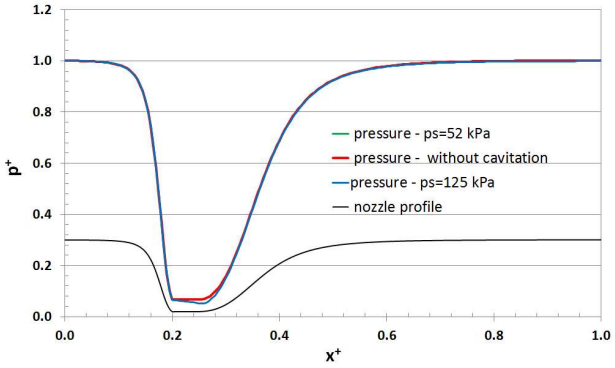

(a) Normalized pressure vs normalized position

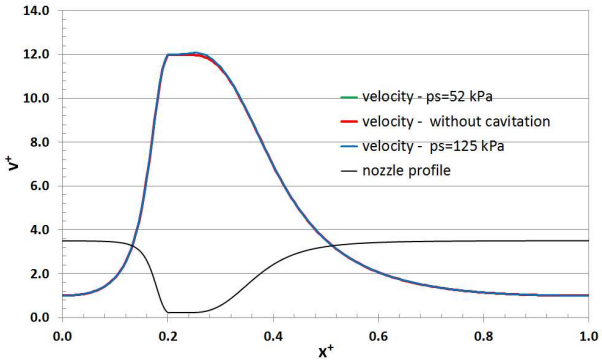

(b) Normalized velocity vs normalized position

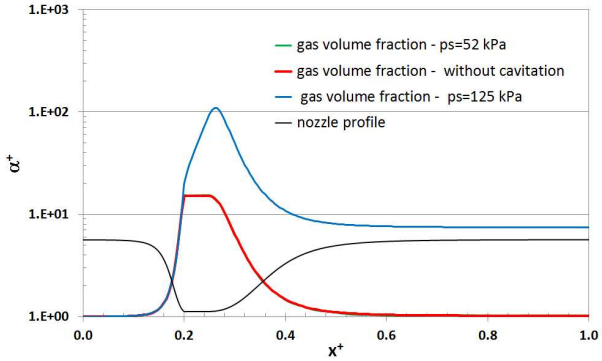

(c) Normalized gas volume fraction vs normalized position

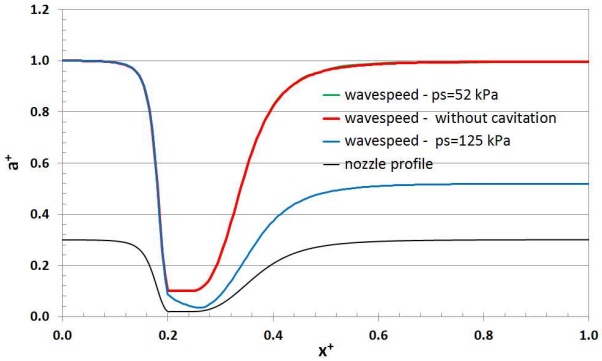

(d) Normalized wavefront speed vs normalized position

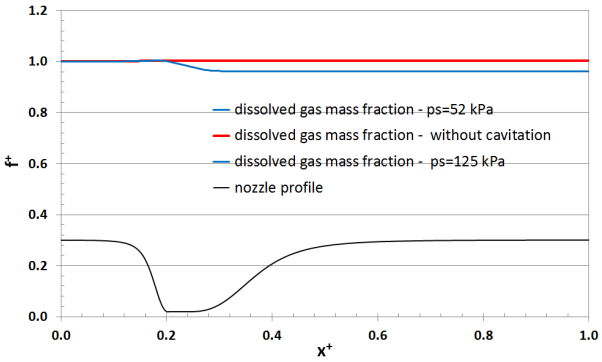

(e) Normalized dissolved gas mass fraction vs normalized position

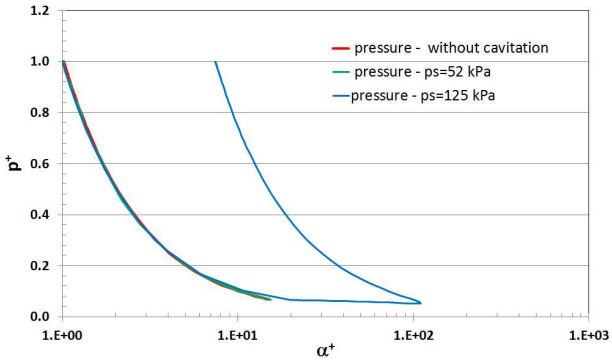

(f) Normalized pressure vs normalized gas volume fraction

Figure 3. Mechanical response of a water-air mixture at room temperature flowing in a converging-diverging nozzle for three different situations: i) without cavitation; ii) with cavitation for a saturation pressure p_s=52 kPa and iii) with cavitation for a saturation pressure p_s=125 kPa. The inlet gas volume fraction is α_o=10^{-4}.

However, in cavitating flows the wavefront speed is reduced of 36% and 96% of its initial value for $p_s = 52$kPa and $p_s = 125$kPa, respectively. Even for $p_s = 125$kPa, the Mach number does not reach values over 0.5. Different from the case for $p_s = 52$kPa, the wavefront speed does not return to its original value of the nozzle inlet. In spite of this, it is possible to see in Fig. 2(e) that the amount of dissolved gas that is released at the nozzle throat is very small (about 4% of its initial value) and is almost the same for for $p_s = 52$kPa and $p_s = 125$kPa. Note that the released gas does not re-dissolves in the liquid in the divergent section. To let in evidence the hysteresis phenomenon induced by the gas release, it has been plotted in Fig. 2(f) the normalized pressure as a function of the normalized gas volume fraction. Since

there is no dissipation at all for the non-cavitating flow, the $p^+ - \alpha+$ path in the convergent section is the same of that in the divergent section, so that the ordinate pair $(p^+, \alpha+)$ in the graphic at the nozzle inlet is the same of that at the nozzle outlet. However, when the gaseous cavitation take places, these two points have distinct coordinates. The greater the saturation pressure is, the more pronounced the hysteresis becomes.

The responses of normalized values of pressure, velocity, gas volume fraction, wavefront speed, dissolved gas mass fraction as a function of the normalized position along the nozzle are depicted in Figs. 3(a), 3(b), 3(c), 3(d), 3(e) for $\alpha_o = 10^{-4}$, for both saturation pressures of $p_s = 52$kPa and $p_s = 125$kPa. As it can be seen in Fig. 3(a) and Fig. 3(b), an increase of α_o of 10000 is not sufficient to alter the pressure and velocity responses, which remain almost equal to that observed for the non-cavitating case. Different from the case in which $\alpha_o = 10^{-8}$, in this new scale there is no perceptible difference between the responses of the gas volume fraction and of the wave front speed between $p_s = 52$kPa and the case without cavitation, as it can be seen in Figs. 3(c) and 3(d). Note that in contrast to the case in which $\alpha_o = 10^{-8}$, significant reduction of the wavefront speed is observed now even when there is no cavitation. However, for the saturation pressure $p_s = 125$kPa significant variations are observed in both the gas volume fraction and in the wave front speed. The maximum absolute value of the gas volume fraction reaches the value of 0.01, whereas the minimum value of the wavefront speed is 100 m/s (with a local Mach number of 0.63), both of them occurring at the nozzle throat. As it has occurred for $\alpha_o = 10^{-8}$, the dissolved gas mass fraction response is indistinguishable for $p_s = 52$kPa and $p_s = 125$kPa as it can be seen in Fig. 3(e). Again, it can be seen that only a small quantity of dissolved gas evolve from the liquid and remains as free gas from the nozzle throat to its outlet. Figure 3(f), which displays the normalized pressure against the normalized gas volume fraction, shows that the hysteresis observed for $p_s = 52$kPa is almost no perceptible since the curve for this saturation pressure is practically superimposed to that in which there is no cavitation. However, for $p_s = 125$kPa it is quite significant.

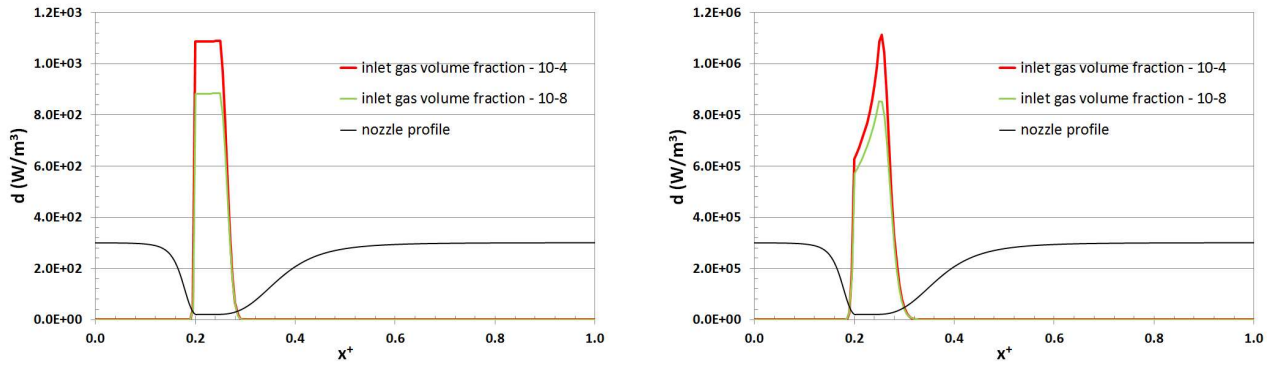

(a) Rate of energy dissipation vs normalized position for p_s=52 kPa

(b) Rate of energy dissipation vs normalized position for p_s=125 kPa

Figure 4. Rate of energy dissipation vs normalized position for a water-air mixture at room temperature flowing in a converging-diverging nozzle for different values of the inlet gas volume fraction α_o=10^{-4} and α_o=10^{-8}.

Finally, it has been presented in Figs. 4(a) and 4(b) the rate of energy dissipation as a function of the normalized position along the nozzle for both values of p_s=52kPa and p_s=125 kPa, respectively. According to the model, the dissipation takes place whenever the pressure falls below the saturation pressure what happens only in the nozzle throat, as it can be seen in Figs. 4(a) and 4(b). While a significant change in the initial volume fraction does not imply in a drastically increase of the rate of dissipation, a small change in the saturation pressure is responsible for increasing the rate of energy dissipation about a factor of 1000. Even though the obtained results seem to be in accordance with which is expected from the physical viewpoint, experimental results are still required to definitively validate the model.

5. FINAL REMARKS

Numerical simulations have been carried out to investigate the influence of the gaseous cavitation on the flow of a air-water mixture through a nozzle. To so so, a thermodynamic coherent model for describing the gas release recently proposed in the literature has been used. In the absence of transonic flows, the mathematical problem is characterized by an initial-value problem formed by a system of ordinary differential equations whose numerical solution has been approximated by employing the well-known Gear's BDF method. The numerical solutions were carried out for two different initial conditions associated with the initial gas volume fraction and two distinct saturations pressures and compared with the case without cavitation. Besides the hysteresis phenomenon observed when the cavitation takes place, it is shown that a small increase in the saturation pressure can drastically increase the rate of energy dissipation and also the behavior of other important variables, such as the wavefront speed.

6. ACKNOWLEDGMENTS

The partial financial support provided by the agencies FAPERJ and CNPq is kindly acknowledged.

7. REFERENCES

Berger, M. S. (1977). *Nonlinearity and Functional Analysis*. Academic Press, London.

Baasiri, M., and Tullis, J. P. (1983). Air release during column separation. *ASME Journal of Fluids Engineering*, *105*, 113–118.

Bergant, A., Simpson, A. R., & Tijsseling, A. R. (2006). Water hammer with column separation: A historical review. *Journal of Fluids and Structures*, *22*, 135–171.

Cannizzaro, D., & Pezzinga, G. (2005). Energy dissipation in transient gaseous cavitation. *ASCE Journal of Hydraulic Engineering*, *131*, (8), 724–732.

Chaudhry, M. H., Bhallamudi, S. M., Martins, C. S., & Naghash, M. (1990). Analysis of transient in bubbly homogeneous, gas-liquid mixtures. *ASME Journal of Fluids Engineering*, *112*, 225–231.

Dorofeeva, I. E., Thomas, F. O., & Dunn, P. F. (2009). Gas release in transient pipe flow. *Proceedings of the 7th International Symposium on Cavitation*, ASME, 1–10, Ann Arbor.

Ekeland, I., & Teman, R. (1976). *Convex Analysis and variational problems*. North-Holland, Amsterdam.

Freitas Rachid, F. B. (2003). A thermodynamicly consistent model for cavitating flows of compressible fluids. *International Journal of Non-Linear Mechanics*, *38*, 1007–1018.

Freitas Rachid, F. B. (2006). Continuum thermo-mechanical model for homogeneous liquidŰgas flows with internal surface tension effects. *Mechanics Research Communications*, *33*, 337-Ű351.

Freitas Rachid, F. B. & Silva, A. B. (2013). Modeling of release and absorption of gas in liquidŰgas flows within a consistent thermodynamic framework. *International Journal of Engineering Science*, *66–67*, 21-Ű43.

Hadj-Taieb, E., & Lili, T. (1998). Transient flow of homogeneous gas-liquid mixtures in pipelines. *International Journal of Numerical Methods for Heat & Fluid Flow*, *8*, (3), 350–368.

Kessal, M., & Bennacer, R. (2005). A new gas release model for a homogeneous liquid-gas mixture flow in pipelines. *International Journal of Pressure Vessels and Piping*, *82*, 713–721.

Kranenburg, C. (1974). Gas release during transient cavitation in pipes. *Journal of the Hydraulics Division*, *100*, (10), 1383–1398.

Moreau, J. J., Panagiotopoulos, P. D., & Strang, G. (1988). *Topics in non-smooth mechanics*. Birkhäuser.

Sander, S., (1999). *Compilation of Henry' s law constants for inorganic and organic species of potential importance in environmental chemistry*. Available at http://www.mpch-mainz.mpg.de/ sander/res/henry.html, accessed in April of 2011.

Swaffiled, J. A. (1972). A study of the influence of air release on column separation in an aviations kerosine pipeline. *Proceedings of the Institution of Mechanical Engineers*, *186*, (56/72), 693–703.

Wylie, E. B. (1984). Simulation of vaporous and gaseous cavitation. *ASME Journal of Fluids Engineering*, *106*, 307–311.

Wylie, E. B., & Streeter, V. L. (1993). *Fluid transients in systems*. Prentice Hall, New York.

Wiggert, D. C., & Sundquist, M. J. (1979). The effect of gaseous cavitation on fluid transients. *ASME Journal of Fluids Engineering*, *101*, 79–86.

Wood, A. B. (1930). *A textbook of sound*. Bell, London.

Zielke, W., Perko, H. D., & Keller, A. (1990). Gas release in transient pipe flow. *Proceedings of the 6th International Conference*, BHRA, 3–14, Cranfield.

8. RESPONSIBILITY NOTICE

The authors are the only responsible for the printed material included in this paper.